

**Manipulative structural re-organization of superficial zone extracellular matrix: articular chondron density increases in response to non-ablation radiofrequency energy**

e-Poster: P154

Congress: ICRS 2010

Type: Electronic Poster

Topic: Basic Science / Physical Stimuli

Authors: K. Ganguly<sup>1</sup>, I.D. McRury<sup>2</sup>, P.M. Goodwin<sup>1</sup>, R.E. Morgan<sup>2</sup>, W.K. Augé<sup>3</sup>; <sup>1</sup>Los Alamos, NM/US, <sup>2</sup>Fall River, MA/US, <sup>3</sup>Santa Fe, NM/US

MeSH:

Cartilage Diseases [C05.182]

Cartilage, Articular [A02.165.407.150]

Tissue Survival [G04.185.908]

Cell Survival [G04.335.316]

**Keywords:** Chondrocyte preservation, Extracellular matrix, Pericellular matrix, Radiofrequency energy

Any information contained in this pdf file is automatically generated from digital material submitted to e-Poster by third parties in the form of scientific presentations. References to any names, marks, products, or services of third parties or hypertext links to third-party sites or information are provided solely as a convenience to you and do not in any way constitute or imply Epilepsy's endorsement, sponsorship or recommendation of the third party, information, product, or service. Epilepsy is not responsible for the content of these pages and does not make any representations regarding the content or accuracy of material in this file.

As per copyright regulations, any unauthorised use of the material or parts thereof as well as commercial reproduction or multiple distribution by any traditional or electronically based reproduction/publication method is strictly prohibited.

You agree to defend, indemnify, and hold Epilepsy harmless from and against any and all claims, damages, costs, and expenses, including attorneys' fees, arising from or related to your use of these pages.

Please note: Links to movies, ppt slideshows and any other multimedia files are not available in the pdf version of presentations.

[www.cartilage.org](http://www.cartilage.org)

## 1. Abstract

**Objective:** Chondron density within the Superficial Zone has been shown to decrease with age, disease, injury, and in response to some interventions and may predispose articular cartilage to extracellular matrix-based failure through an inability to support the mechanotransductive demands of physiologic loading. Since chondron shape and orientation reflect inter-territorial extracellular matrix architecture, chondron density is an important descriptor for functional cartilage. Interventions that alter chondron density may provide insight into the treatment outcome of focal lesions. This study evaluated radiofrequency energy effects on native Superficial Zone chondron density in articular cartilage demonstrating early lacunar emptying without significant surface fibrillation.

**Design:** Radiofrequency energy was delivered by two methods for both 5 second and 10 second durations to ex-vivo femoral condyle osteochondral specimens obtained from patients undergoing total joint replacement; Ablation and Non-Ablation. Untreated control and treated specimens were sectioned, prepared with Live/Dead cell viability stain, and assessed by confocal fluorescence laser microscopy. **Results:** The mean total Superficial Zone cell number in control sections was 1480 per  $\text{mm}^2$ . The Ablation method fully corrupted the Superficial Zone by volumetric loss or near complete cellular necrosis with a mean post-treatment depth of necrosis of the remaining residual cartilage at the treatment site of 140  $\mu\text{m}$  (range 104  $\mu\text{m}$  - 199  $\mu\text{m}$ ) at 5 seconds and 226  $\mu\text{m}$  at 10 seconds (range 140  $\mu\text{m}$  - 334  $\mu\text{m}$ ) through the Transitional Zone tissue. The Non-Ablation method retained the

Superficial Zone with a mean total number of cells of 1468 per  $\text{mm}^2$  (no statistical difference from control) with a 12% increase in live chondron density of over control ( $p < 0.02$ ). Chondrocyte viability, intra-chondron chondrocyte geographic pattern, chondron image character, and the Transitional Zone was not altered in the non-ablation treatment group; the increased live chondron density partially originated from preferential extracellular matrix volume contraction of the Superficial Zone.

**Conclusions:** This report suggests that non-ablative radiofrequency energy can preferentially increase articular cartilage Superficial Zone live chondron density. The Superficial Zone extracellular matrix, because of its distinctive composition, is uniquely suited to manipulative structural reorganization. Resetting functional chondron density patterns may have the potential to create a more chondro-supportive environment for articular cartilage as it inherently responds to focal disease.

## 2. Purpose

Articular cartilage disease constitutes a large burden for our population which needs to be addressed with practical socioeconomic solutions<sup>(1-5)</sup>. Because articular cartilage has offered surface changes as the first readily diagnosable visual and tactile cue of its degeneration, the orthopedic surgeon has been given the responsibility of first responder<sup>(6-9)</sup>. This responsibility has led to the limited adoption of mechanical shavers and thermal or plasma ablation devices as a viable treatment for early articular cartilage disease due to the collateral damage and lesion progression they can cause<sup>(7)</sup>. The opportunity to achieve successful early surgical intervention for articular cartilage lesions rather than waiting for full-thickness lesions to develop has recently been made possible with the advent of non-ablation radiofrequency technology<sup>(10, 11)</sup>.

Non-ablation radiofrequency technology enables the selective targeting and removal of the damaged tissue associated with early articular cartilage disease without causing necrosis in the contiguous cartilage tissue surrounding the lesion<sup>(10)</sup>. This is accomplished by a protected electrode architecture (Figure 1) that prohibits electrode-to-tissue contact so that the resistive tissue heating and tissue electrolysis induced by electrical current and associated with tissue necrosis do not occur like in thermal and plasma ablation devices. The protective housing creates a primary reaction zone that is shielded from the large physical fluid-flow and convective forces present during surgical application

enabling deployment of low-level radiofrequency energy to create low-energy physiochemical conversions that can be used for surgical work. A repetitive molecular energy conversion loop under non-ionizing electromagnetic forces is created wherein the rapid splitting and reconstitution of the water molecule occurs. A sister technology to the fuel cell that harnesses energy from the molecular bonds of water, these physiochemical conversions create products that are concentrated through techniques such as capacitive deionization and concentration enrichment and delivered to the treatment site in a controlled and localized fashion through precipitation, sedimentation, thermal, or chemical gradient forces via redox magnetohydrodynamic fluid flow<sup>(11)</sup>. Thermal and plasma ablation devices have exposed electrodes making any attempt at low-energy physiochemical conversions inconsequential due to the large physical fluid-flow and convective forces present during surgical application; hence, their design necessitates a large amount of energy delivery to the treatment site that leads to collateral damage around the tissue target.

Non-ablation radiofrequency treatments are a surface-based intervention useful for surface-based conditions such as early articular cartilage damage. The low-level energy delivery is configured to modify/precondition diseased articular cartilage to a state amenable to a safe and effective gentle mechanical débridement with the protective housing leading edge. The non-ablation radiofrequency energy products effect the accessible and degenerate surface matrix structure of damaged cartilage tissue preferentially rather than the intact chondron and matrix tissue deep to the surface lesion level. In this manner, the non-ablation energy takes advantage of the altered pericellular and extracellular matrices of diseased cartilage<sup>(12-21)</sup> by preparing damaged tissue for subsequent débridement with the protective housing leading edge through augmented and/or naturally facile tissue cleavage patterns<sup>(10)</sup>. As early articular cartilage disease manifests as matrix failure, non-ablation radiofrequency technology creates a matrix-failure-based intervention that corresponds to cartilage biology.

The matrix failure of surface fibrillation remains an attractive therapeutic target for early surgical intervention modalities<sup>(7)</sup>. By safely removing diseased surface fibrillation that serves as both a mechanical stress riser and a source of biologic load that propagate damage<sup>(19-30)</sup>, these lesions can be stabilized<sup>(10)</sup>. Lesion stabilization remains a necessary prerequisite toward articular cartilage tissue preservation since a residually healthy lesion site is an essential substrate for permitting or inducing effective healing responses. It has been demonstrated (see Figure 2) that Superficial Zone characteristics with viable chondrocytes can be preserved during the targeted removal of surface fibrillation<sup>(10)</sup>. Since the area adjacent to surface fibrillation often exhibits a soft character as noted by tactile cues<sup>(7)</sup>, it would be useful if this tissue could be treated concurrent with the surface fibrillation whereby such a procedure would serve both as a therapeutic intervention for the tactile soft lesion and as a defined safety margin during the targeting of surface fibrillation lesions.

Chondron density has been shown to decrease with age, disease, injury, and in response to some interventions and may predispose articular cartilage to extracellular matrix-based failure through an inability to support the mechanotransductive demands of physiologic loading<sup>(12, 13)</sup>. Since chondron shape and orientation reflect inter-territorial extracellular matrix architecture, chondron density is an important descriptor for functional and degenerating cartilage<sup>(12, 13, 31, 32)</sup>. Interventions that alter chondron density through matrix modification may provide insight into the treatment outcome of focal lesions. We have shown previously (see Figure 2) that chondron density with live chondrocytes preferentially increases within the residual Superficial Zone after targeted removal of surface fibrillation with non-ablation radiofrequency techniques<sup>(10)</sup>. This study evaluates both ablation (thermal and plasma ablation) and non-ablation radiofrequency energy effects on

native Superficial Zone chondron density in articular cartilage that demonstrates early lacunar emptying without significant surface fibrillation.

### 3. Methods and Materials

Osteochondral femoral condyle specimens were harvested from patients undergoing total knee replacement under an approved Institutional Review Board protocol. Specimens were included that demonstrated an area of uniform tactile soft chondromalacia adjacent to areas of surface fibrillation (partial thickness damage) of sufficient size from which test samples could be obtained that demonstrated geographically similar characteristics. After harvest, specimens were divided and each part was randomly sequestered into a treatment group and immediately transferred to an ex vivo arthroscopic treatment setting. Three treatment groups were established with a part from each specimen; Control (which received no treatment), Ablation (thermal and plasma ablation), and Non-Ablation.

Each treatment group was assigned its own station with an ex vivo arthroscopy set-up. Standard arthroscopic fluid was used at room temperature with a fluid-flow rate of 30cc/min  $\pm$  5cc/min which created consistent fluid dynamics in the set-up typical of in vivo arthroscopy. The flow was measured and recorded at each station throughout the study and was maintained constant for all testing. The radiofrequency systems were used at the generator settings recommended by their manufacturer's design<sup>(10)</sup>: thermal and plasma Ablation included Glider<sup>®</sup> (Smith and Nephew, Inc.; Andover, Massachusetts) and Paragon<sup>®</sup> (Arthrocare, Inc.; Austin, Texas); Non-Ablation included Ceruleau<sup>®</sup> (NuOrtho Surgical, Inc.; Fall River, Massachusetts).

Treatment of the tactile soft cartilage surfaces was performed by one practicing surgeon accustomed to radiofrequency débridement chondroplasty. The goal of the treatment was to utilize the same technique typically deployed to remove fibrillated cartilage and smooth the articular surface as determined by visual cues. Energy delivery treatment time was divided into 5 and 10 second groups with a technique of moving the probe tip back and forth at the treatment site with a consistent application pressure and speed as judged by the surgeon to mimic in vivo treatment conditions. With the ablation devices, the surgeon used the active electrode as a mechanical implement for gentle electrode contact, consistent with their design, by moving the electrode across the articular surface during the allotted energy deposition time. With the Non-Ablation system, the surgeon used the protective housing edge to mechanically brush the surface of the tissue concurrent with energy delivery for the allotted treatment time. Immediately after each treatment, three 0.5 mm coronal sections of each sample were obtained referencing the center of the treatment site. The sections were prepared for staining by washing in HEPES buffered saline solution. Live/Dead<sup>®</sup> Reduced Biohazard Cell Viability Kit #1 green and red fluorescence, SKU #L-7013, (Invitrogen™, Carlsbad, California) was used per manufacturer's specification to stain specimens. Specimens were glutaraldehyde fixed, transferred to standard flat glass slides, and flooded with VectaShield<sup>®</sup> fluorescence protection oil prior to the placement of #1.5 borosilicate glass cover slips over each specimen section.

Confocal fluorescence laser microscopy analysis was performed by personnel blinded to the identity of the treatment groups for each specimen part. Confocal imaging was performed with an Olympus IX-81 inverted microscope coupled to an Olympus FV300 confocal laser scanning unit (Center Valley, Pennsylvania, USA) using 488 nm laser excitation. Live cells were captured under green fluorescent channel (505-525 nm) and dead cells were captured under red fluorescent channel (577-634 nm), generating a Live image, a Dead image, and an Integrated Live/Dead image.

The extent of collateral damage induced by each treatment was determined based upon both the amount of initially non-damaged cartilage tissue removed from the treatment site when compared to control specimens and the condition of the residual tissue remaining at the treatment site. Depth of

necrosis of the residual tissue post-treatment for both the 5 and 10 second groups was determined by measuring the distance from the center of the residual tissue surface after treatment to the lowest depth of dead cells observed. Total number of cells, number of dead cells, and number of live cells per  $\text{mm}^2$  were counted for the treatment site of each group. Chondrocyte geographic profile (i.e. single, pairs, strings, or clusters) and chondron image character (i.e. shape, dimension, lacunar fill, orientation) were compared between Group specimens and between pre-and post-treatment specimens by combining patterns into comparable categories. Chondron density was determined both by quantifying cell populations per  $\text{mm}^2$  in two-dimensional section images integrated at the tissue surface and by measuring inter-chondron distances. These calculations were designed to accommodate the problem of volumetric tissue ablation extraction observed with ablation devices (10), and therefore included counts and measurements spanning the Superficial and Transitional Zones, if present, at the tissue surface. Multiple range ANOVA analysis and two sided t-tests were performed for differences in depth of cartilage tissue necrosis, number of chondrocytes, and chondron population for each group.

#### 4. Results

Six patients yielding six separate specimens were included for study, generating twenty-four osteochondral parts tested. Residual post-treatment tissue characteristics varied significantly between the treatment groups (Figure 3).

The Control specimens demonstrated tactile soft surfaces adjacent to areas of surface fibrillation consistent with gross visual inspection of the harvested tissues. Early lacunar emptying was evident mostly limited to the surface portion of the Superficial Zone (Figure 4). Chondrocytes with a flattened chondron appearance typical of this zone remained present within the tactile soft surfaces with chondrocyte geographic patterns including singles, pairs, strings, and clusters as noted in Figure 3. Live cells were abundantly present in chondrons in and around the tactile soft areas exhibiting lacunar emptying with evidence of chondrocyte depletion and some dead cell populations mostly at surface positions ( $<13\%$  per  $\text{mm}^2$ ). Cell population densities within each specimen group remained constant as the sample parts of each group originated from the same specimen. Inter-specimen comparisons did not reveal significant differences in relative cell population density, chondrocyte geographic profile, chondron image character, or inter-chondron distance confirming similar lesion type included for study.

The Ablation specimens demonstrated large charred tissue segments, generalized gelatinization of tissue indicative of altered matrix properties, and loss of cartilage thickness above that of control throughout the treatment site. Tissue charring ranged from light-brownish color to near black or dark grey indicating severe char and tissue damage for the thermal ablation specimens. The gelatinized tissue was observed to have a semi-translucent appearance and much softer consistency than the surrounding cartilage in the plasma ablation specimens. Areas of tissue fragmentation indicating ablation extraction as is typically observed during standard electrocautery procedures were evident for both the thermal and plasma ablation specimens (Figure 5). No treated specimens yielded either a visually or histologically smooth cartilage surface when compared to control. The tissue surface was replaced with a residual layer of necrotic and damaged tissue in all instances completely eliminating Superficial Zone characteristics due to volumetric tissue loss exceeding the level of disease pre-treatment (Figure 3). Consequently, evaluations of Superficial Zone chondrons was not possible at the treatment site. Cellular density, geographic chondrocyte profile, chondron image character, and inter-chondron distance of the residual tissue under the necrotic layer depicted an altered and damaged Transitional Zone when compared to control specimens (Insert A). Dead cells were present in all specimens independent of chondrocyte geographic profile and occasionally intermixed with live cells to a varying degree (Insert B). As depicted in Figure 6, the mean post-treatment depth of necrosis

was 140  $\mu\text{m}$  (range 104  $\mu\text{m}$  - 199  $\mu\text{m}$ ) at 5 seconds and 226  $\mu\text{m}$  at 10 seconds (range 140  $\mu\text{m}$  - 334  $\mu\text{m}$ ) through the residual Transitional Zone tissue (as distinct from necrosis through Superficial Zone tissue as this Zone had been volumetrically removed due to ablation tissue extraction).

The Non-Ablation specimens demonstrated a smooth residual surface at the treatment site with no areas of charred, gelatinized, or color altered tissue and without bulk tissue loss. All specimens retained intact Superficial Zone characteristics in the residual tissue at the treatment site (Figure 3). The chondrocyte geographic pattern and chondron image character of the retained Superficial Zone were not altered over control, with live chondrocytes persisting independent of their geographic profile (Insert C). Live cells were evident throughout the treatment site with chondrocytes residing closer to the surface and with a general decrease in inter-chondron measurement when compared to Control. This finding indicated a relative increase in surface-based cellularity post-treatment in the retained Superficial Zone of the treatment site. Areas of lacunar emptying and chondrocyte depletion evident in the Control specimens were generally not present. The Transitional Zone did not demonstrate altered cell density pattern, geographic chondrocyte profile, inter-chondron measurement, or evidence of cellular death. As depicted in Figure 6, no areas of necrosis or dead cells were observed at 5 seconds and only one treatment sample demonstrated any cell death at 10 seconds. In that sample, 3% of cells were found dead up to 67  $\mu\text{m}$  deep limited to the Superficial Zone.

Figure 7 displays the comparison of cell counts for each treatment Group. Because of the volumetric tissue loss that occurred in the Ablation group, the comparison depicted is between the Control specimens with a Superficial Zone, the Ablation specimens without a Superficial Zone and an exposed Transitional Zone, and the Non-Ablation specimens with a retained Superficial Zone. The mean total cell number in Control sections was 1480 per  $\text{mm}^2$ . Even though the Ablation method fully corrupted the Superficial Zone, the mean total cell number in the residual Transitional Zone tissue was 1546 per  $\text{mm}^2$  (no statistical difference from control;  $p < 0.92$ ); yet, with a decreased live cell density of 36% over control ( $p < 0.02$ ) without necrosis preference relative to chondrocyte geographic profile within the chondrons. The Non-Ablation method which retained Superficial Zone characteristics demonstrated a mean total number of cells of 1468 per  $\text{mm}^2$  (no statistical difference from control;  $p < 0.92$ ) with increased live cell density of 12% over control ( $p < 0.02$ ) independent of geographic chondrocyte profile within the chondrons. Cell count remained consistently proportional to chondron count throughout the sections. The decreased live chondron density of the Ablation group reflected primarily an increased cellular necrosis induced in the residual tissue commensurate with the volumetric ablation extraction of the tissue surfaces; whereas, the increased live chondron density of the Non-Ablation group reflected both a preferential extracellular matrix volume contraction whereby additional live cells were brought into the surface quantification area and a small cleavage plane surface removal of diseased Superficial Zone tissue (Figure 8). Multiple range ANOVA analysis demonstrated a statistically significant difference between the depth of cartilage tissue necrosis ( $p < 0.004$ ) and percent chondrocyte death ( $p < 0.003$ ) between the Ablation group and the Non-Ablation group.

## 5. Conclusions

This study demonstrates that non-ablation radiofrequency energy can be used to preferentially increase the density of live chondrons in the Superficial Zone independent of geographic chondrocyte profile and without causing cellular necrosis in tactile soft articular cartilage displaying early lacunar emptying adjacent to fibrillated lesions. These findings are similar to those we reported previously in the residual tissue after targeted removal of surface fibrillation where Superficial Zone characteristics were retained and chondron density with live chondrocytes was increased without an increase in dead chondrocytes<sup>(10)</sup>. This study demonstrates that the effects of Non-Ablation radiofrequency energy as characterized by confocal live/dead fluorescence laser microscopy can be limited to the Superficial

Zone matrix with no evidence of decreased cellular viability or of alterations in geographic chondrocyte profile, chondron image character, or the Transitional Zone. These effects partly reflect a relative preferential extracellular matrix (ECM) modification through a volume contraction; and, provide confirmation of a defined safety margin qualified to the targeting of surface fibrillation lesions with non-ablation radiofrequency techniques. Since this study evaluated two dimensional integrated images from the tissue surface, it remains unknown whether the matrix modification of ECM volume contraction is disparate in the x, y, and z coordinates. As others have observed a uniform chondron-to-matrix density pattern<sup>(31, 32)</sup>, suggesting that biologic constraints exist to maintain tissue integrity against the development of focal matrix-failure lesions, resetting functional chondron density patterns in early lesions may have the potential to create a more chondro-supportive environment for articular chondrocytes<sup>(12, 13, 31, 32)</sup> as they inherently pursue matrix maintenance<sup>(13)</sup> and respond to focal disease<sup>(33)</sup>.

Consistent with numerous previous studies<sup>(for review see 7, 10)</sup>, and even though safer than mechanical shavers, thermal and plasma ablation treatments fully corrupted the Superficial Zone, both the matrix and cellular structures, with electrocautery-like tissue extraction, leaving an exposed and damaged Transitional Zone in place of the original tactile soft Superficial Zone. Since the control group exhibited significant live chondrocyte populations in the Superficial Zone, this study provides further evidence that thermal and plasma ablation treatments do not have a role in early intervention for articular cartilage lesions. Volumetric tissue loss can only contribute to articular cartilage lesion progression by converting a potentially salvageable lesion with Superficial Zone characteristics to one that may not be salvageable with an exposed and damaged Transitional Zone that can lead to accelerated wear<sup>(19-30)</sup>. Unnecessarily induced volumetric tissue loss and cellular necrosis has been deemed inappropriate for an early intervention strategy; rather, the interest in treating early cartilage disease is that based upon tissue biology.

For the surgeon, the earliest visual and tactile cues of articular cartilage degeneration reside in the Superficial Zone, causing this anatomic region to be an appropriate focus for early intervention strategies and placing it into a crucial role for articular cartilage tissue preservation. Because of its distinctive structure and composition, the Superficial Zone is uniquely suited as a therapeutic surgical target from both a diagnostic and a cell-matrix perspective. The Superficial Zone has several layers of varying degree disc-shaped flattened chondrocytes within a matrix of densely packed bundles of thin collagen and elastin fibers oriented parallel-oblique to the articular surface with relatively low proteoglycan content<sup>(20, 34, 35)</sup>. These layers can serve as physical delamination or cleavage planes between damaged and undamaged areas<sup>(20, 21)</sup> that can be exploited to stabilize lesions once matrix failure begins to manifest in the most superficial layers<sup>(10)</sup>. Left untreated and as lesions progress to exhibit further matrix disruption, the resident chondrocytes lose the ability to maintain tissue integrity<sup>(13)</sup>; conversely, stabilized lesions that preserve Superficial Zone characteristics and viable chondrocytes can retain the healing potential of this zone's cellular phenotype. For a matrix modification procedure to hold relevance for early intervention, preserving viable chondrocytes after lesion stabilization remains important. Further studies by our team with non-ablation radiofrequency energy designed to treat early articular cartilage lesions have verified no decrease in chondrocyte viability post-treatment when bulk tissue specimens were incubated for 96 hours (unpublished data).

The Superficial Zone chondrocyte population retains unique cellular properties depicting a healing phenotype potential that is paramount to maintain in an early intervention approach to articular cartilage disease. The chondrocyte geographic distribution within Superficial Zone chondrons occurs in distinct patterns with horizontal chondron alignment<sup>(36)</sup>, consistent with this zone's matrix

structure of cleavage planes<sup>(20, 21)</sup>, rendering it amenable to targeted lesion stabilization from a cellular perspective<sup>(7, 10)</sup>. When compared to other zonal phenotypes, these chondrocytes demonstrate differences in metabolism<sup>(37)</sup>, in chondron morphology<sup>(38)</sup>, in geographic distribution throughout the matrix based upon anatomic location<sup>(39)</sup>, and in gene expression producing zone-specific molecules like clusterin, proteoglycan 4, and lubricin. The Superficial Zone has been implicated as a driver of chondrocyte migration in response to focal partial-thickness lesions<sup>(33)</sup>, zonal reorganization<sup>(40)</sup>, appositional growth<sup>(41, 42)</sup>, chondroproliferation<sup>(43)</sup>, chondrocyte colony formation<sup>(41)</sup>, and a side population source of mesenchymal progenitor cells<sup>(41, 44, 45)</sup> that express stem cell markers<sup>(41, 46)</sup>, contractile actin isoforms<sup>(47)</sup>, progenitor cell signaling mediators<sup>(46, 48, 49)</sup>, and monolayer expansion behavior while maintaining a chondrogenic phenotype<sup>(41)</sup>. Treatments that eliminate the Superficial Zone chondrocyte population, like mechanical shavers and thermal or plasma ablation devices, can leave residual Transitional Zone chondrocytes and their accompanying matrix exposed to physiologic demands for which they are not designed to accommodate. Further, a damaged and exposed Transitional Zone does not retain the healing phenotype potential evident within the Superficial Zone chondrocyte population and unnecessarily places an iatrogenic burden upon tissue contiguous to the lesion.

Aside from exploiting the mechanical cleavage patterns inherent in the Superficial Zone of early disease for lesion stabilization<sup>(10, 20, 21, 36)</sup>, theoretical matrix modification of the Superficial Zone without damage to the chondrocyte and chondron has been considered possible due to this zone's unique matrix properties. Articular chondrocytes are surrounded by a protective layer, the pericellular matrix (PCM), which is thought to function as a non-linear mechanical filter that modulates the physiochemical and biomechanical environments experienced by chondrocytes through processes like transmembrane signaling<sup>(50-57)</sup>. The PCM displays distinct biomechanical properties when compared to the ECM<sup>(51, 54)</sup>. For example, the Young's modulus of the PCM is uniform with tissue depth in that it is similar to the ECM modulus of the Superficial Zone but significantly lower than the ECM modulus of the Transitional and Deep Zones<sup>(14, 15, 54, 55, 57)</sup>. This disparity in properties, or stiffness ratio<sup>(56)</sup>, allows the chondrocyte environment to be more consistent when confronted with large incongruities in local zone- and region-specific ECM forces<sup>(52, 53, 55, 57)</sup>. The PCM may protect the micromechanical environment of the chondrocyte in regions of high local strain such as in the Superficial Zone and may amplify lower magnitudes of local strain such as those occurring in the Transitional Zone<sup>(50, 54)</sup>. Further, the fluid permeability of PCM relative to the ECM is much lower allowing the functional phasic properties of the ECM during loading to be shielded from the chondrocyte<sup>(55)</sup>. These unique properties would allow the chondron and chondrocyte in the Superficial Zone to accommodate alterations in the ECM with a protective PCM posture; whereas once the Transitional Zone chondron and chondrocyte are exposed to a surface-level environment due to acute damage or disease, the PCM of the Transitional Zone may amplify the increased ECM strains witnessed by the Transitional Zone's new surface locale to a detrimental level for both the chondrocyte and matrix. These PCM properties may partially explain the retention of viable chondrocytes in the Superficial Zone after non-ablation radiofrequency energy application; as well as, the significant disease progression that can be induced by mechanical shavers and thermal or plasma ablation devices that create an exposed and damaged Transitional Zone that is then subjected to repetitive physiologic loading.

The matrix modification induced by non-ablation radiofrequency applications appears to be a relative ECM rather than a predominant PCM phenomenon histologically. The PCM collagen structure, like its

mechanical properties<sup>(54, 55, 57)</sup>, is uniform with tissue depth in articular cartilage, while the ECM displays zonal and regional inhomogeneities<sup>(21, 56)</sup>. The PCM in articular cartilage is generally defined by the exclusive presence of type VI collagen defining its boundary with the ECM. Type VI collagen exhibits unique properties which play important roles in mediating cell-matrix and intermolecular interactions. In articular cartilage, type VI collagen serves as an extracellular adhesion molecule that forms a network anchoring the chondrocyte cell membrane to the PCM through its interaction with other extracellular matrix molecules like hyaluronan, biglycan, perlecan, heparin, decorin, and fibronectin. Type VI collagen is responsible for the structural integrity and mechanical properties, like stiffness, of the PCM<sup>(58)</sup>; and, it can self-assemble into disulfide-bonded dimers and tetramers leading to a distinctive thin-beaded filamentous network around cells<sup>(59)</sup>. Type VI collagen consists of three different  $\alpha$ -chains and contains a Kunitz-type proteinase inhibitor sequence in the  $\alpha 3$  chain rendering it resistant to proteolysis<sup>(60)</sup>. In general, the triple helical conformation of collagen is lost when its temperature exceeds 37<sup>0</sup> C; but, interestingly, there is evidence that Type VI collagen is partially resistant to heating up to 70<sup>0</sup> C<sup>(61)</sup>, is only denatured by heating to 90<sup>0</sup> C in the presence of reducing agents<sup>(61)</sup>, and is resistant to depolymerization<sup>(62)</sup>. These structural nuances help to explain why the PCM appears in this study to be less vulnerable to physiochemical matrix modification than the ECM which is composed primarily of type II collagen and aggrecan. Chondron viability may be protected during a matrix modification that appears to lead chondrons into an increased density pattern by Superficial Zone ECM volume contraction.

Although osteoarthritic changes in the PCM and ECM mechanotransductive properties have been shown to alter the mechanical environment of the chondrocyte, it remains unclear whether the PCM and ECM properties change in a disparate fashion during disease progression<sup>(17, 18, 55)</sup>; and, how these changes might correlate to the relative matrix failure of early articular cartilage disease. Characterizing these changes will assist in developing matrix modifications that are sensitive to the changes in cell-to-matrix relationships that may alter the stress-strain and fluid-flow environment of the chondrocyte<sup>(55)</sup>. Because the water volume fraction in articular cartilage is critically dependent upon the function of the Superficial Zone in modulating drag forces, Superficial Zone chondron density continues to be a relevant parameter of functional cartilage as degenerative changes are assessed. The biologic role of structural matrix alterations has been the subject of recent modeling studies<sup>(17, 18)</sup>. Additional attention toward the lamina splendens is also important<sup>(20, 34, 35)</sup>, particularly due to the unique role its interwoven collagen network plays in modulating proteoglycan content and subadjacent collagen network orientation<sup>(20)</sup> that is accessible during Superficial Zone lesion stabilization. The observation that chondrocytes adhere to areas of lamina splendens disruption<sup>(63)</sup> and the combined biomechanical effects of wear-line and split-line orientation<sup>(64)</sup> warrant further investigation for early intervention strategies.

This study evaluated tactile soft articular cartilage displaying decreased chondron density associated with early lacunar emptying and a small non-viable cell population concentrated in its Superficial Zone. Chondrocyte depletion, whether by apoptosis, necrosis, or other mechanisms<sup>(65)</sup>, may be a predisposing condition to surface fibrillation as noted in the adjacent regions of the tissue harvested for this study. As shown in Figure 2, surface fibrillation often demonstrates intact chondrons within the fibrillation itself, with extruded chondrocytes uncommonly noted in areas within and around the surface fibrillation<sup>(7, 10)</sup>. This data provides some evidence that overt ECM failure rather than primary PCM failure is the early condition presented to the surgeon for treatment consideration. Early intervention remains attractive particularly since full-thickness lesions have received significant attention and may be the next opportunity for which tissue preserving intervention might be

considered. Interestingly, a confluence of cell-to-matrix interaction research has been observed through the treatment of articular cartilage with electromagnetic energy. Chondrocyte proliferation, gene expression modification, temporal changes in matrix production, and lacuna formation in response to single exposure electromagnetic fields <sup>(66)</sup> has been shown, which is consistent with observations of a cartilage response to voltage potential delivery at the disease locale of full-thickness defects <sup>(67)</sup>. Our team has observed similar findings (see Figure 9) in that these clinical responses occur more reliably for margin-intact lesions, implicating the resident Superficial Zone in the healing response observed for full-thickness lesions (unpublished data). These responses might serve as a target substrate for non-destructive electromagnetic energy induced host-to-implant lateral integration as an adjunct to implant-to-host approaches pursued for full-thickness defects <sup>(68)</sup>. Not only does the healing potential phenotype of the Superficial Zone provide treatment substrate options for Superficial Zone and full-thickness lesions, it may also provide additional treatment substrate options for Transitional Zone lesions surrounded by an intact Superficial Zone.

## 6. References

1. Curl WW, Krome J, Gordon ES, Rushing J, Smith BP, Poehling GG. Cartilage injuries: a review of 31,516 knee arthroscopies. *Arthroscopy* 1997; 13:456-460.
2. Hjelle K, Solheim E, Strand T, Muri R, Brittberg M. Articular cartilage defects in 1,000 knee arthroscopies. *Arthroscopy* 2002; 18:730-734.
3. Moskowitz RW. The burden of osteoarthritis: clinical and quality-of-life issues. *Am J Manag Care* 2009; 15(suppl):S223-229.
4. Widuchowski W, Widuchowski J, Trzaska T. Articular cartilage defects: study of 25,124 knee arthroscopies. *Knee* 2007; 14:177-182.
5. Woolf AD, Pfleger B. Burden of major musculoskeletal conditions. *Bull World Health Organ* 2003; 81:646-656.
6. Bekkers EJ, Creemers LB, Dhert WJA, Saris DBF. Diagnostic modalities for diseased articular cartilage--from defect to degeneration: a review. *Cartilage* 2010; 1: 157-164.
7. Ganguly K, McRury ID, Goodwin PM, Morgan RE, Augé WK. Native chondrocyte viability during cartilage lesion progression: normal to surface fibrillation. *Cartilage*; July 22, 2010 as doi:10.1177/1947603510373918.
8. Joshi NS, Bansal PN, Stewart RC, Snyder BD, Grinstaff MW. Effect of contrast agent charge on visualization of articular cartilage using computed tomography: exploiting electrostatic interactions for improved sensitivity. *J Am Chem Soc* 2009 Sep 23; 131(37):13234-13235.
9. Smolinski D, Jones CW, Wu JP, Miller K, Kirk TB, Zheng MH. Confocal arthroscopic assessment of osteoarthritis in situ. *Arthroscopy* 2008 Apr; 24(4):423-429.
10. Ganguly K, McRury ID, Goodwin PM, Morgan RE, Augé WK. Histopomorphic evaluation of radiofrequency mediated débridement chondroplasty. *Open Orthop J* 2010; 4:211-220.
11. McRury ID, Morgan RE, Augé WK. The manipulation of water with non-ablation radiofrequency energy: a repetitive molecular energy conversion loop under non-ionizing electromagnetic forces. 2010; in review.

12. Aigner T, Haag J, Martin J, Buckwalter J. Osteoarthritis: aging of matrix and cells--going for a remedy. *Curr Drug Targets* 2007 Feb; 8(2):325-331.
13. Aigner T, Söder S, Gebhard PM, McAlinden A, Haag J. Mechanisms of disease: role of chondrocytes in the pathogenesis of osteoarthritis--structure, chaos and senescence. *Nat Clin Pract Rheumatol* 2007 Jul; 3(7):391-399.
14. Alexopoulos LG, Haider MA, Vail TP, Guilak F. Alterations in the mechanical properties of the human chondrocyte pericellular matrix with osteoarthritis. *J Biomechanical Engineering Trans ASME* 2003; 125:323-333.
15. Alexopoulos LG, Williams GM, Upton ML, Setton LA, Guilak F. Osteoarthritic changes in the biphasic mechanical properties of the chondrocyte pericellular matrix in articular cartilage. *J Biomechanics* 2005; 38:509-517.
16. Hollander AP, Pidoux I, Reiner A, Rorabeck C, Bourne R, Poole AR. Damage to type II collagen in aging and osteoarthritis starts at the articular surface, originates around chondrocytes, and extends into the cartilage with progressive degeneration. *J Clin Invest* 1995; 96:2859-2869.
17. Kim E, Guilak F, Haider MA. The dynamic mechanical environment of the chondrocyte: a biphasic finite element model of cell-matrix interactions under cyclic compressive loading. *J Biomech Eng* 2008 Dec; 130(6):061009.
18. Kim E, Guilak F, Haider MA. An axisymmetric boundary element model for determination of articular cartilage pericellular matrix properties in situ via inverse analysis of chondron deformation. *J Biomech Eng* 2010 Mar; 132(3):031011.
19. Temple-Wong MM, Bae WC, Chen MQ, Bugbee WD, Amiel D, Coutts RD, Lotz M, Sah RL. Biomechanical, structural, and biochemical indices of degenerative and osteoarthritic deterioration of adult human articular cartilage of the femoral condyle. *Osteoarthritis Cartilage* 2009; 17(11):1469-1476.
20. Wu JP, Kirk TB, Zheng MH. Study of the collagen structure in the superficial zone and physiological state of articular cartilage using a 3D confocal imaging technique. *J Orthop Surg Res* 2008 Jul 17; 3-29.
21. Saarakkala S, Julkunen P, Kiviranta P, Mäkitalo J, Jurvelin JS, Korhonen RK. Depth-wise progression of osteoarthritis in human articular cartilage: investigation of composition, structure and biomechanics. *Osteoarthritis Cartilage* 2010 Jan; 18(1):73-81.
22. Broom ND, Ngo T, Tham E. Traversing the intact/fibrillated joint surface: a biomechanical interpretation. *J Anat* 2005; 206:55-67.
23. Choi JB, Youn I, Cao L, Leddy HA, Gilchrist CL, Setton LA, Guilak F. Zonal changes in the three-dimensional morphology of the chondron under compression: the relationship among cellular, pericellular, and extracellular deformation in articular cartilage. *J Biomech* 2007; 40:2596-2603.
24. Flachsmann R, Kim W, Broom N. Vulnerability to rupture of the intact articular surface with respect to age and proximity to site of fibrillation: a dynamic and static-investigation. *Connect Tissue Res* 2005; 46:159-169.
25. Glaser C, Putz R. Functional anatomy of articular cartilage under compressive loading: quantitative aspects of global, local and zonal reactions of the collagenous network with respect to the surface integrity. *Osteoarthritis Cartilage* 2002; 10:83-99.

26. Kerin AJ, Coleman A, Wisnom MR, Adams MA. Propagation of surface fissures in articular cartilage in response to cyclic loading in vitro. *Clin Biomech (Bristol, Avon)* 2003; 18:960-968.
27. Lewis JL, Johnson SL. Collagen architecture and failure processes in bovine patellar cartilage. *J Anat* 2001; 199(pt 4):483-492.
28. Papaioannou G, Demetropoulos CK, King YH. Predicting the effects of knee focal articular surface injury with a patient-specific finite element model. *Knee* 2010; 17:61-68.
29. Setton LA, Zhu W, Mow VC. The biphasic poroviscoelastic behavior of articular cartilage: role of the surface zone in governing the compressive behavior. *J Biomech* 1993; 26:581-592.
30. Silver FH, Bradica G, Tria A. Do changes in the mechanical properties of articular cartilage promote catabolic destruction of cartilage and osteoarthritis? *Matrix Biol* 2004; 23:467-476.
31. Treweek AJ, Please CP, Landman KA. A continuum model for the development of tissue-engineered cartilage around a chondrocyte. *Math Med Biol* 2009 Sep; 26(3):241-262.
32. Quinn TM, Hunziker EB, Häuselmann HJ. Variation of cell and matrix morphologies in articular cartilage among locations in the adult human knee. *Osteoarthritis Cartilage* 2005 Aug; 13(8):672-678.
33. Roluffs B, Williams JM, Aurich M, Grodzinsky AJ, Kuettner KE, Cole AA. Proliferative remodeling of the spatial organization of human superficial chondrocytes distant from focal early osteoarthritis. *Arthritis Rheum.* 2010 Feb; 62(2):489-498.
34. Mansfield J, Yu J, Attenburrow D, Moger J, Tirlapur U, Urban J, Cui Z, Winlove P. The elastin network: its relationship with collagen and cells in articular cartilage as visualized by multiphoton microscopy. *J Anat* 2009 Dec; 215(6):682-691.
35. Yu J, Urban JP. The elastic network of articular cartilage: an immunohistochemical study of elastin fibres and microfibrils. *J Anat* 2010 Apr; 216(4):533-541.
36. Roluffs B, Williams JM, Grodzinsky AJ, Kuettner KE, Cole AA. Distinct horizontal patterns in the spatial organization of superficial zone chondrocytes of human joints. *J Struct Biol* 2008 May; 162(2):335-344.
37. Fukui N, Ikeda Y, Ohnuki T, Tanaka N, Hikita A, Mitomi H, Mori T, Juji T, Katsuragawa Y, Yamamoto S, Sawabe M, Yamane S, Suzuki R, Sandell LJ, Ochi T. Regional differences in chondrocyte metabolism in osteoarthritis: a detailed analysis by laser capture microdissection. *Arthritis Rheum* 2008; 58:154-163.
38. Youn I, Choi JB, Cao L, Setton LA, Guilak F. Zonal variations in the three-dimensional morphology of the chondron measured in situ using confocal microscopy. *Osteoarthritis Cartilage* 2006; 14:889-897.
39. Schumacher BL, Su JL, Lindley KM, Kuettner KE, Cole AA. Horizontally oriented clusters of multiple chondrons in the superficial zone of ankle, but not knee articular cartilage. *Anat Rec* 2002 Apr 1; 266(4):241-248.
40. Hayes AJ, Hall A, Cheung I, Brown L, Tubo R, Caterson B. Surface zone but not deep zone chondrocytes reorganize zonal architecture of articular cartilage grafts grown in vitro. *Trans Orthop Res Soc.* Vol.30, Poster 1774, Washington, D.C., 2005.
41. Dowthwaite GP, Bishop JC, Redman SN, Khan IM, Rooney P, Evans DJ, Houghton L, Bayram Z, Boyer S, Thomson B, Wolfe MS, Archer CW. The surface of articular cartilage contains a progenitor cell population. *J Cell Sci* 2004; 117:889-897.

42. Hayes AJ, MacPherson S, Morrison H, Dowthwaite G, Archer CW. The development of articular cartilage: evidence for an appositional growth mechanism. *Anat Embryol (Berl)* 2001; 203:469-479.
43. Grogan SP, Olee T, Hiraoka K, Lotz MK. Repression of chondrogenesis through binding of notch signaling proteins HES-1 and HEY-1 to N-box domains in the COL2A1 enhancer site. *Arthritis Rheum* 2008; 58:2754-2763.
44. Hattori S, Oxford C, Reddi AH. Identification of superficial zone articular chondrocyte stem/progenitor cells. *Biochem Biophys Res Commun* 2007; 358:99-103.
45. Martin JM, Smith M, Al-Rubeai M. Cryopreservation and in vitro expansion of chondroprogenitor cells isolated from the superficial zone of articular cartilage. *Biotechnol Prog* 2005; 21:168-177.
46. Grogan SP, Miyaki S, Asahara H, D'Lima DD, Lotz MK. Mesenchymal progenitor cell markers in human articular cartilage: normal distribution and changes in osteoarthritis. *Arthritis Res Ther* 2009; 11(3):R85.
47. Kim AC, Spector M. Distribution of chondrocytes containing alpha-smooth muscle actin in human articular cartilage. *J Orthop Res* 2000 Sep; 18(5):749-755.
48. Hayes AJ, Dowthwaite GP, Webster SV, Archer CW. The distribution of notch receptors and their ligands during articular cartilage development. *J Anat* 2003 Jun; 202(6):495-502.
49. Karlsson C, Lindahl A. Articular cartilage stem cell signaling. *Arthritis Res Ther* 2009; 11:121.
50. Choi JB, Youn I, Cao L, Leddy HA, Gilchrist CL, Setton LA, Guilak F. Zonal changes in the three-dimensional morphology of the chondron under compression: the relationship among cellular, pericellular, and extracellular deformation in articular cartilage. *J Biomech* 2007; 40(12):2596-2603.
51. Guilak F, Alexopoulos LG, Upton ML, Youn I, Choi JB, Cao L, Setton LA, Haider MA. The pericellular matrix as a transducer of biomechanical and biochemical signals in articular cartilage. *Ann N Y Acad Sci* 2006 Apr; 1068:498-512.
52. Korhonen RK, Herzog W. Depth-dependent analysis of the role of collagen fibrils, fixed charges and fluid in the pericellular matrix of articular cartilage on chondrocyte mechanics. *J Biomech* 2008; 41(2):480-485.
53. Korhonen RK, Julkunen P, Wilson W, Herzog W. Importance of collagen orientation and depth-dependent fixed charge densities of cartilage on mechanical behavior of chondrocytes. *J Biomech Eng.* 2008 Apr; 130(2):021003.
54. Guilak F, Alexopoulos LG, Haider MA, Ting-Beall HP, Setton LA. Zonal uniformity in mechanical properties of the chondrocyte pericellular matrix: micropipette aspiration of canine chondrons isolated by cartilage homogenization. *Ann Biomed Eng* 2005; 33:1312-1318.
55. Alexopoulos LG, Setton LA, Guilak F. The biomechanical role of the chondrocyte pericellular matrix in articular cartilage. *Acta Biomater.* 2005 May; 1(3):317-325.
56. Julkunen P, Wilson W, Jurvelin JS, Korhonen RK. Composition of the pericellular matrix modulates the deformation behaviour of chondrocytes in articular cartilage under static loading. *Med Biol Eng Comput* 2009 Dec; 47(12):1281-1290.
57. Darling EM, Wilusz RE, Bolognesi MP, Zauscher S, Guilak F. Spatial mapping of the biomechanical

properties of the pericellular matrix of articular cartilage measured in situ via atomic force microscopy. *Biophys J* 2010 Jun 16; 98(12):2848-2856.

58. Alexopoulos LG, Youn I, Bonaldo P, Guilak F. Developmental and osteoarthritic changes in Col6a1-knockout mice: biomechanics of type VI collagen in the cartilage pericellular matrix. *Arthritis Rheum* 2009 Mar; 60(3):771-779.

59. Eyre D. Collagen of articular cartilage. *Arthritis Res* 2002; 4(1):30-35.

60. Jansen ID, Hollander AP, Buttle DJ, Everts V. Type II and VI collagen in nasal and articular cartilage and the effect of IL-1alpha on the distribution of these collagens. *J Mol Histol* 2010 Feb; 41(1):9-17.

61. Hesse H, Engvall E. Type VI collagen. Studies on its localization, structure, and biosynthetic form with monoclonal antibodies. *J Biol Chem* 1984 Mar 25; 259(6):3955-3961.

62. Spissinger T, Engel J. Type VI collagen beaded microfibrils from bovine cornea depolymerize at acidic pH, and depolymerization and polymerization are not influenced by hyaluronan. *Matrix Biol* 1995 Feb; 14(6):499-505.

63. Secretan C, Bagnall KM, Jomha NM. Effects of introducing cultured human chondrocytes into a human articular cartilage explant model. *Cell Tissue Res* 2010 Feb; 339(2):421-427.

64. Bae WC, Wong VW, Hwang J, Antonacci JM, Nugent-Derfus GE, Blewis ME, Temple-Wong MM, Sah RL. Wear-lines and split-lines of human patellar cartilage: relation to tensile biomechanical properties. *Osteoarthritis Cartilage* 2008 Jul;16(7): 841-845.

65. Almonte-Becerril M, Navarro-Garcia F, Gonzalez-Robles A, Vega-Lopez MA, Lavallo C, Kouri JB. Cell death of chondrocytes is a combination between apoptosis and autophagy during the pathogenesis of osteoarthritis within an experimental model. *Apoptosis* 2010 May; 15(5):631-638.

66. Chang CH, Loo ST, Liu HL, Fang HW, Lin HY. Can low frequency electromagnetic field help cartilage tissue engineering? *J Biomed Mater Res A* 2010 Mar 1; 92(3):843-851.

67. Voloshin I, Morse KR, Allred CD, Bissell SA, Maloney MD, DeHaven KE. Arthroscopic evaluation of radiofrequency chondroplasty of the knee. *Am J Sports Med* 2007; 35(10):1701-1707.

68. Khan IM, Gilbert SJ, Singhrao SK, Duance VC, Archer CW. Cartilage integration: evaluation of the reasons for failure of integration during cartilage repair. A review. *Eur Cell Mater* 2008 Sep 3; 16:26-39.

## 7. Author Information

Kumkum Ganguly, PhD <sup>1</sup>; Ian D. McRury, PhD <sup>2</sup>; Peter M. Goodwin, PhD <sup>3</sup>; Roy E. Morgan, PE <sup>2</sup>; Wayne K. Augé II, MD <sup>2, 4</sup>

1 B-Division, Los Alamos National Laboratory; Los Alamos, New Mexico, USA

2 NuOrtho Surgical, Inc.; Fall River, Massachusetts, USA

3 Center for Integrated Nanotechnologies, Los Alamos National Laboratory; Los Alamos, New Mexico, USA

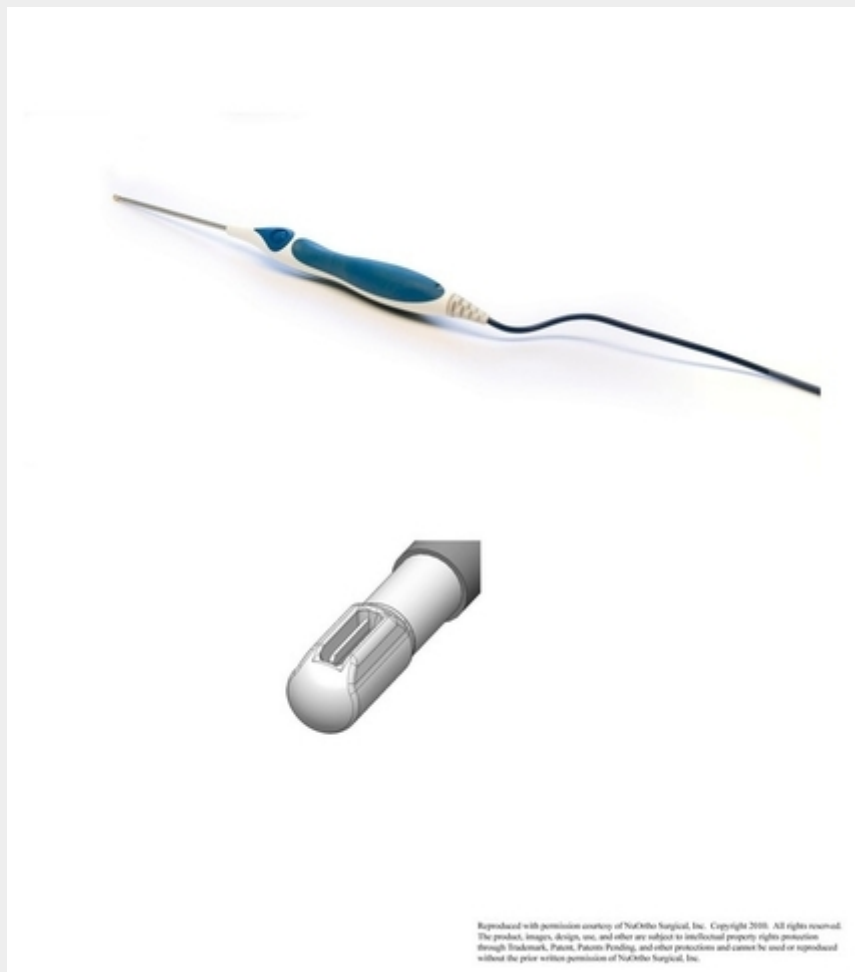
4 Center for Orthopaedic and Sports Performance Research, Inc.; Santa Fe, New Mexico, USA

Acknowledgements: The work was performed at the Center for Integrated Nanotechnologies, United States Department of Energy, Office of Basic Energy Sciences User Facility, Los Alamos National Laboratory, Los Alamos, New Mexico (Contract DE-AC52-06NA25396) and Sandia National

Laboratories (Contract DE-AC04-94AL85000) and Physicians Medical Center, Santa Fe, New Mexico. This study was supported by the New Mexico Small Business Grant Program WNM700, RO31, Los Alamos National Laboratory, Los Alamos, New Mexico and by NuOrtho Surgical, Inc., Fall River, Massachusetts.

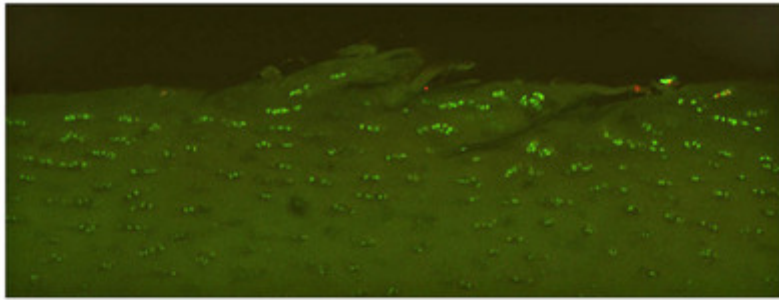
## 8. Mediafiles

**Figure 1. A Non-Ablation Radiofrequency Device.**

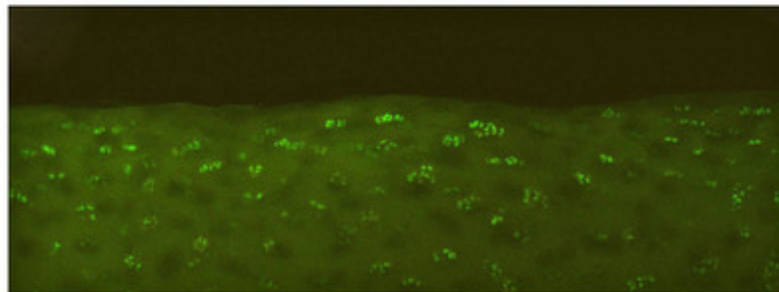


The active electrode is encased by a protective housing that prohibits electrode-to-tissue contact and creates a primary reaction zone that is shielded from the large physical fluid-flow and convective forces present during surgical application. This architecture eliminates the resistive tissue heating and tissue electrolysis associated with the tissue necrosis induced by thermal and plasma ablation devices and enables the use of low-energy physiochemical conversions to be deployed for surgical work. Ceruleau®.

**Figure 2. Targeted Removal of Surface Fibrillation.**



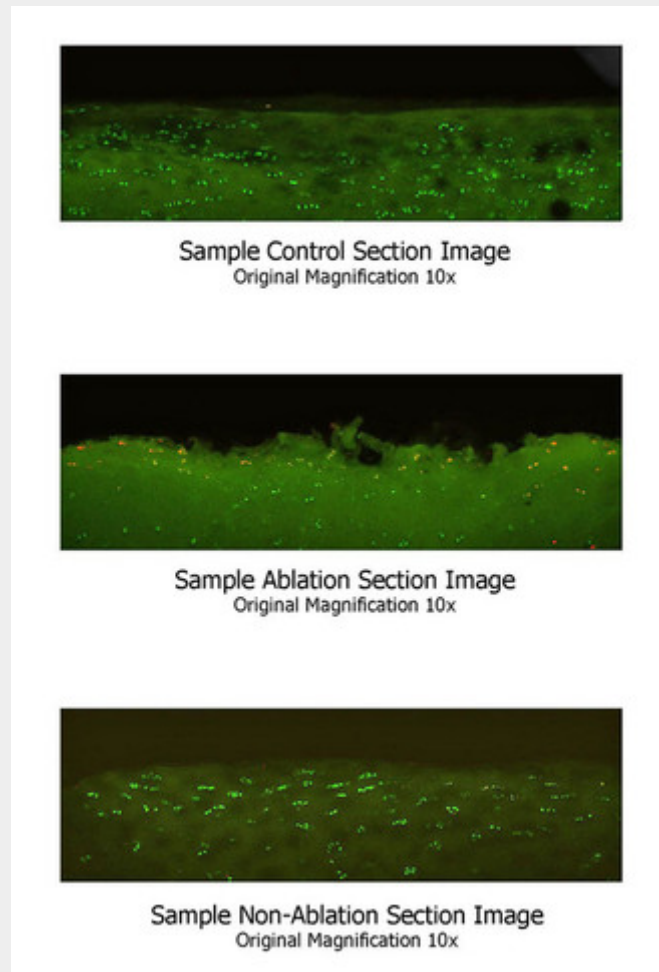
Sample Section Image of Surface Fibrillation  
Original Magnification 10x



Sample Section Image Post-Treatment  
Original Magnification 10x

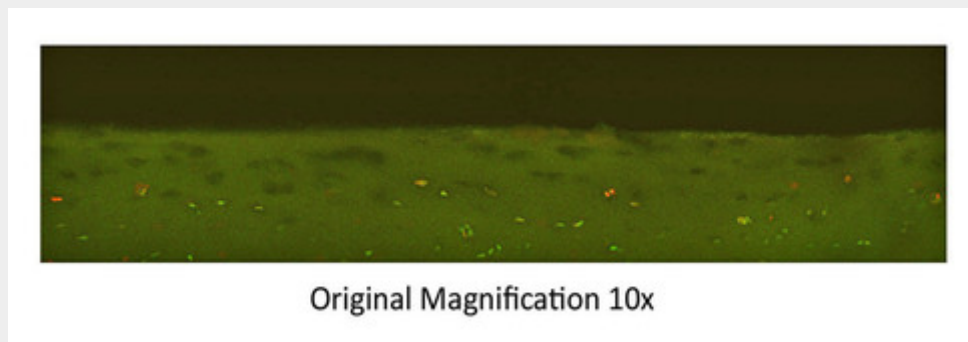
Representative pre- and post-treatment integrated Live/Dead cell viability stain section images demonstrating targeted removal of surface fibrillation without inducing necrosis in the contiguous tissue at the treatment site. The non-ablation radiofrequency energy modifies/preconditions the altered pericellular and extracellular matrices of diseased cartilage, preparing it for subsequent débridement with the protective housing leading edge through augmented and/or naturally facile tissue cleavage patterns.

**Figure 3. Group Comparison of Section Images.**



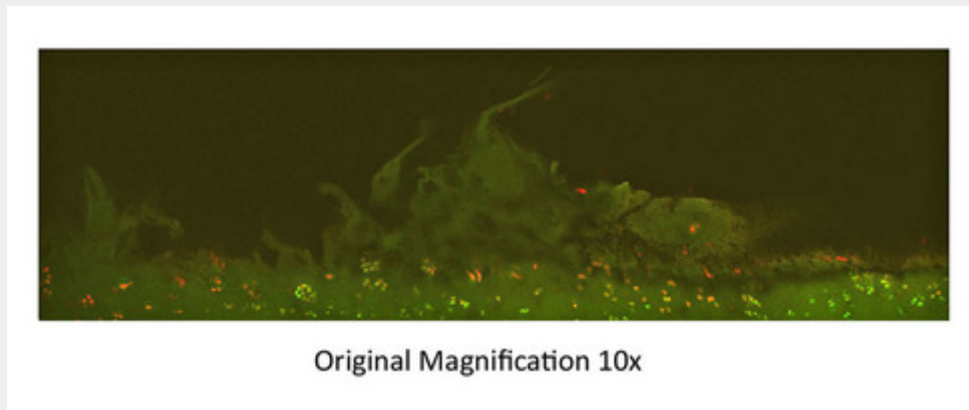
Representative integrated Live/Dead cell viability stain section images depicting the comparative structural reorganization of the Superficial Zone of tactile soft articular cartilage. Note the increased live surface chondron density of the Non-Ablation section and the ablation extraction of the Superficial Zone and resulting Transitional Zone exposure of the Ablation section.

**Figure 4. Enlarged Control Group Section Image.**



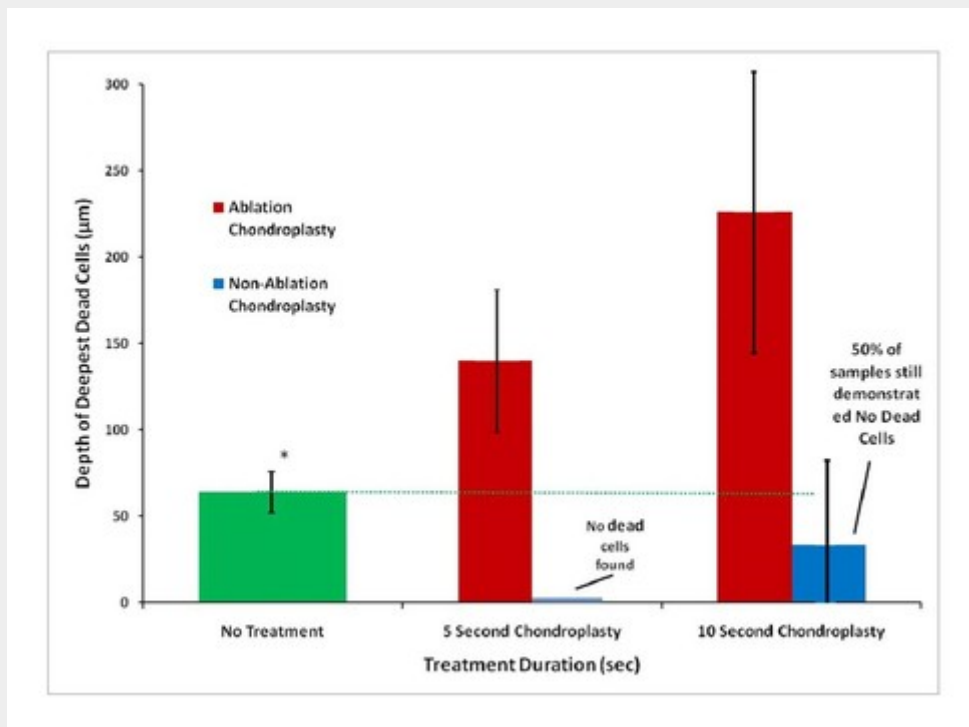
Representative integrated Live/Dead cell viability stain section image demonstrating early lacunar emptying with a small population of non-viable chondrocytes in the region.

**Figure 5. Enlarged Ablation Group Section Image.**



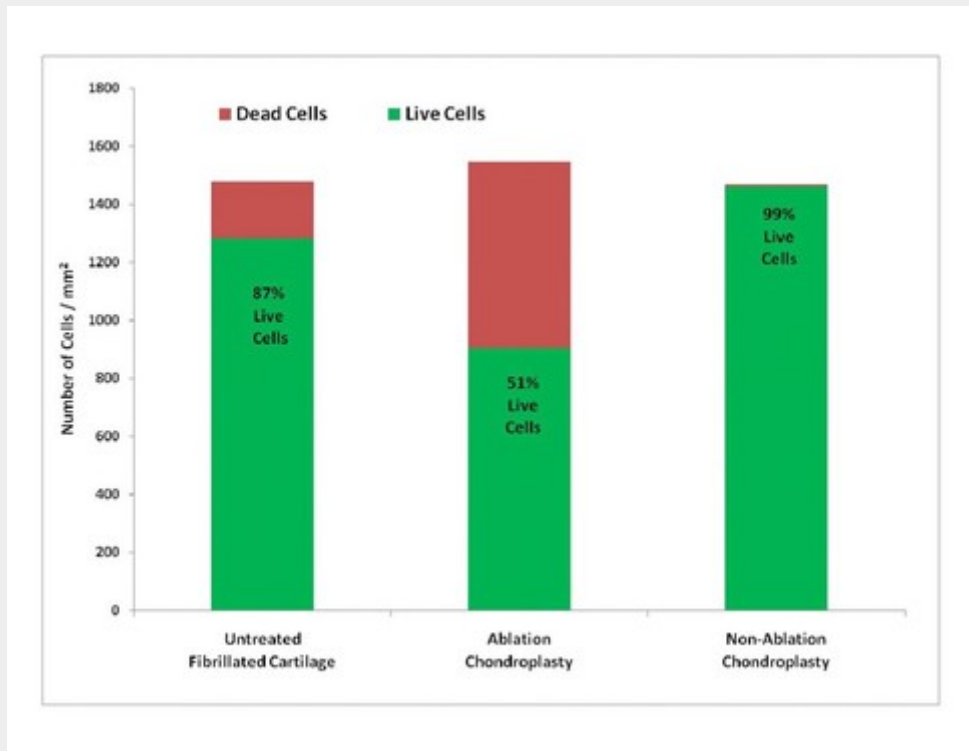
Representative integrated Live/Dead cell viability stain section image demonstrating ablation tissue extraction and corresponding non-viable chondrocytes.

**Figure 6. Depth of Necrosis Comparison between Groups.**



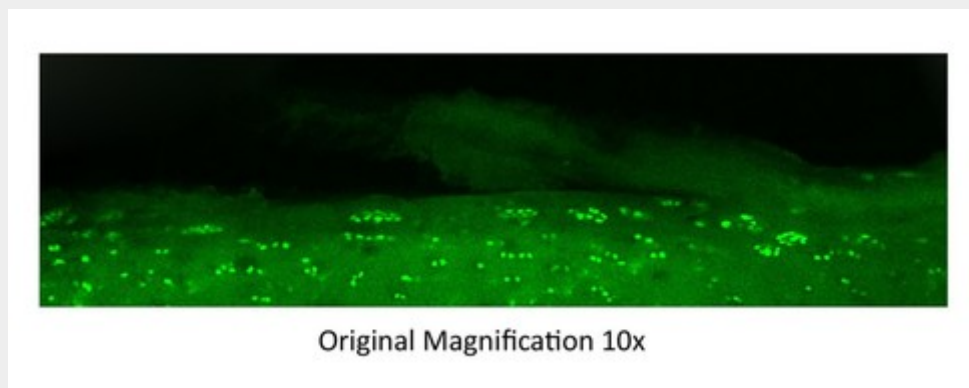
Depth of necrosis noted by dead chondrocytes versus duration of treatment. Note that the Ablation Group depicts Transitional Zone tissue due to volumetric tissue ablation extraction of the Superficial Zone; while the Control and Non-Ablation Groups retain Superficial Zone characteristics for depth of necrosis measurement.

**Figure 7. Cell Count Comparison between Groups.**



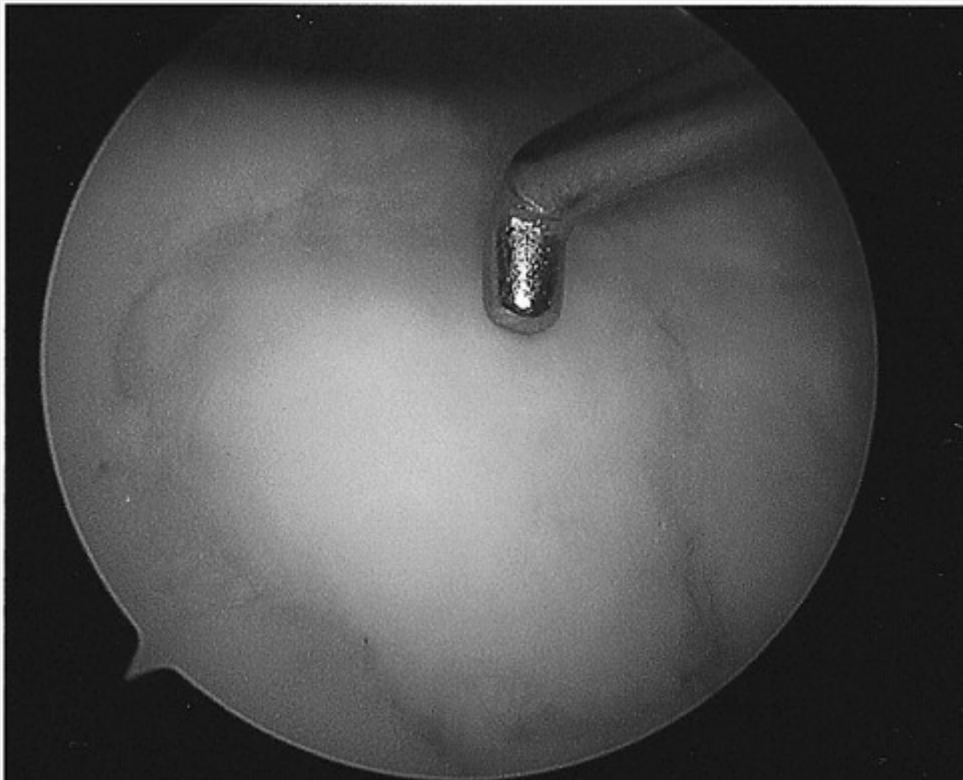
Total number of cells, number of live cells, and number of dead cells noted within the residual tissue post-treatment. Note that the Ablation specimens did not exhibit Superficial Zone characteristics due to ablation extraction of the tissue with the cell counts exclusive to the Transitional Zone.

**Figure 8. Enlarged Section Image of Superficial Zone Cleavage Plane.**



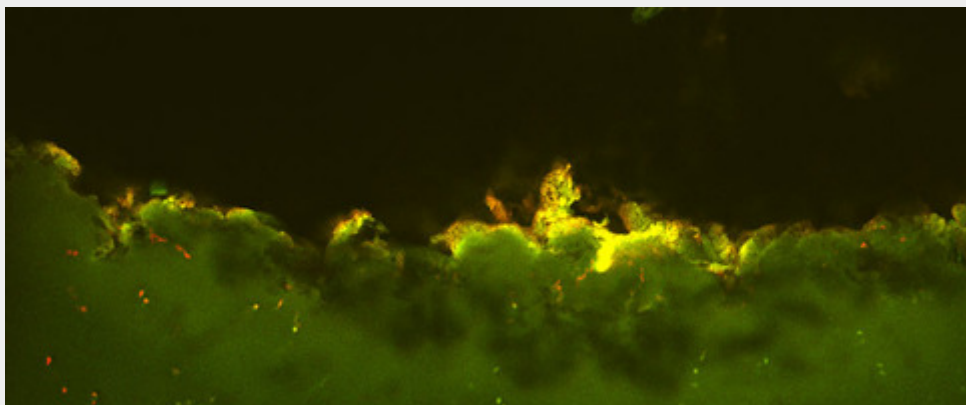
Representative cell viability stain section image demonstrating the surface physical delamination or cleavage planes that can be exploited for targeted intervention during lesion stabilization.

**Figure 9. Intra-Operative Photograph during Second-Look Arthroscopy.**



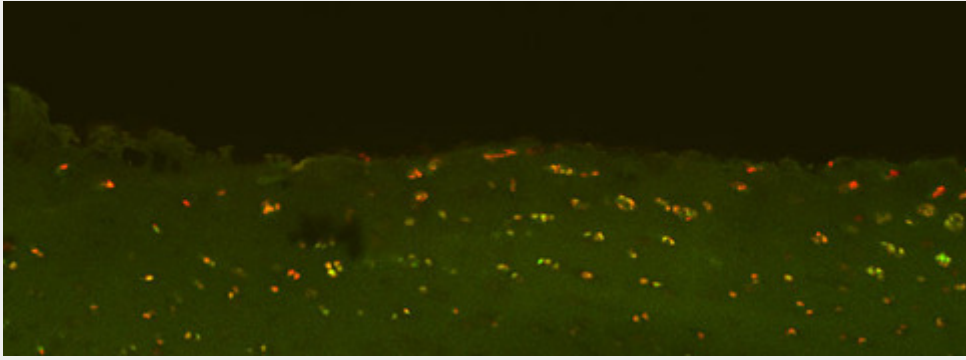
Healing response noted upon second-look arthroscopy at 357 days from the index procedure. The initial lesion was a stable full-thickness margin-intact femoral trochlea defect treated with a targeted constant alternating current voltage potential of 240V at 460kHz applied to the lesion margins without current deposition for 10 seconds.

**Insert A. Ablation Induced Transitional Zone Alterations.**



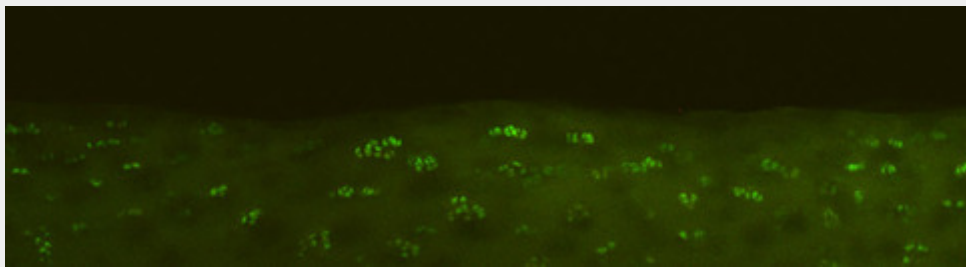
Representative integrated Live/Dead cell viability stain section image depicting the residual Transitional Zone after treatment with Ablation radiofrequency energy for 5 seconds. Original Magnification 10x.

**Insert B. Chondrocyte Geographic Profile after Ablation Treatment.**



Representative integrated Live/Dead cell viability stain section image depicting ablation chondrocyte death at the margin of treatment site damage still depicting Superficial Zone characteristics. Note that chondrocyte death is independent of chondrocyte geographic profile of single, pairs, strings, or clusters. Original magnification 10x.

**Insert C. Chondrocyte Geographic Profile after Non-Ablation Treatment.**



Representative integrated Live/Dead cell viability stain section image depicting live chondrocytes post-treatment independent of chondrocyte geographic profile of singles, pairs, strings, or clusters. Original magnification 10x.